Journal of Engineering and Technology

ISSN 2180-3811 eISSN 2289-814X https://jet.utem.edu.my/jet/index

THE STUDY OF KINEMATICS AND TRAJECTORY PLANNING OF A 9-DOF SERIAL REDUNDANT ROBOTIC MANIPULATOR

W. K. Chee[1] and T. F. Chay[*1]

[1] Faculty of Engineering and Technology,
Tunku Abdul Rahman University of Management and Technology, Jalan Genting Kelang, Setapak, 53300 Kuala Lumpur, Malaysia.

corresponding: chaytf@tarc.edu.my

Article history:
Received Date: 25 January 2024
Revised Date: 5 March 2024
Accepted Date: 8 May 2024

Keywords:
Inverse Kinematics, Redundant Robotic Manipulator, Industrial Robots

Abstract— A serial manipulator exhibits kinematic redundancy when the number of dimensions in its joint space exceeds that of its end-effector space. This paper proposes a solution to resolve the redundancy issue in a 9-Degree-of-Freedom (DOF) serial manipulator. The solution involves segmenting the robot's kinematic model into two sections: a 3-DOF base (axes 1-3) and a 6-DOF body (axes 4-9). Denavit-Hartenberg (D-H) parameters and homogeneous transformation matrices are used to formulate the forward kinematics equations for both sections. Subsequently, the inverse kinematics solutions for each section are derived using the Jacobian

pseudo-inverse method. The proposed method's effectiveness is tested by commanding the base and body sections of the 9-DOF manipulator to follow two independent trajectories simultaneously, demonstrating its ability to generate dexterous motions. An experiment to assess the manipulator's capability to maneuver its end-effector along a specified path while its redundant links follow another, all while avoiding obstacles in a constrained environment is conducted. The results show that the end-effector and redundant links successfully track their respective trajectories with minimal position error and no collisions with the obstacle. In conclusion, the proposed method has been successfully demonstrated to effectively address the kinematic redundancy problem in a 9-DOF serial manipulator.

I. Introduction

A. Research Background

Robotic manipulators are extensively employed in various industrial sectors due to their ability to complete tasks without human intervention. They frequently handle automated tasks like pick-and-place applications, automated welding, painting, palletizing, assembly operations, etc. A serial robotic manipulator, also known as an open-chain kinematic system, consists of a series of connected mechanical links. These links are joined by motor-actuated joints and culminate in an end-effector. This end-effector often takes the form of a tool or device designed to interact with other objects. In mechanics, degrees-of-freedom (DOF) refer to the minimum number of coordinates needed to define a robot's configuration. Essentially, the

number of DOF corresponds to the robot's configuration space [1].

Robotic manipulators can be classified into two types, non-redundant manipulator and redundant manipulator depending on the dimension of the joint space and the end-effector space. A robotic manipulator is said to be kinematically redundant when the dimension of joint space is greater than the dimension of the end-effector space [2]. Non-redundant manipulators have only one joint configuration for a given end-effector pose. This means that when the manipulator places the end-effector in the desired pose, its body is fixed and lacks the freedom to move. It must adopt the specific joint configuration necessary to achieve that precise end-effector position. This limits the manipulator's flexibility in positioning the end-effector. Further complicating matters, robotic manipulators sometimes need to fulfil multiple tasks simultaneously, such as a primary task to move the end-effector to a desired position and orientation, while a secondary task to move its body for obstacle avoidance. In these situations, a non-redundant manipulator cannot fulfil all the requirements at the same time due to its limited flexibility. This is where redundant manipulators come in.

With their additional degrees of freedom, redundant manipulators can achieve the same end-effector pose through countless joint configurations. This offers them greater flexibility in performance and dexterity compared to non-redundant manipulators. Furthermore, redundancy empowers the manipulator to perform secondary tasks like obstacle avoidance while maintaining the desired end-effector pose, overcoming the limitations of non-redundant manipulators.

B. Problem Statement

Commonly used industrial robots include 6-DOF articulated robots, 4-DOF SCARA robots, 1 to 4-DOF Cartesian robots, and 5 to 7-DOF collaborative robots

(cobots). A 6-DOF articulated robot can freely move its end-effector in all 6 degrees of freedom, including translational movement along the X-Y-Z axes in Cartesian space and rotational movement about the X-Y-Z axes. This means the robot can place its end-effector at any desired pose within its workspace. However, in some industrial applications, these robots may not be optimal when robots need to perform additional actions like obstacle or collision avoidance between their bodies and other objects (secondary task) while concurrently moving their end-effector (primary task). This paper proposes a 9-DOF serial redundant robotic manipulator with three redundant axes to address these limitations and investigate its potential for improved obstacle avoidance using its kinematic redundancy.

C. Research Objective

This paper aims to study the kinematics and trajectory planning algorithms for a 9-DOF serial redundant robotic manipulator. To achieve this goal, the following objectives are formulated:

a) Design a 9-DOF serial redundant robotic manipulator in SolidWorks

b) Formulate the forward and inverse kinematics algorithms of the 9-DOF manipulator using Jacobian-based iterative method.

c) Formulate a trajectory planning algorithm for the manipulator that includes trajectories for both the end-effector and the redundant axes.

d) Verify and demonstrate the formulated algorithms through simulations involving obstacle avoidance, and various desired end-effector trajectories, using a suitable simulation platform.

II. Literature Review

A. Concept and Theory

Serial robotic manipulators are composed of a series of connected links that can move only in one direction, forming an open kinematic chain [3]. Forward kinematics in these manipulators involves computing the position and orientation of the end-effector based on the values of each joint variable and the length of each

link. While this can be solved with geometric methods using trigonometry, the Denavit-Hartenberg (D-H) parameter approach with homogeneous transformation matrices is preferred for complex robots. Inverse kinematics, essentially the opposite of forward kinematics, determines the joint configuration needed to place the end-effector at a desired position and orientation. Two main methods for solving inverse kinematics are analytical and iterative [4]. For complex or redundant manipulators, analytical solutions might not exist, making iterative methods like the Jacobian-based iterative method a common approach. This method uses a locally linear approximation of the nonlinear system at a given point, represented by the Jacobian matrix, a matrix consisting of first-order partial derivatives of the functions defining the relationship between joint angles and end-effector pose:

$$\boldsymbol{J} = \frac{\partial \boldsymbol{f}}{\partial \boldsymbol{\theta}} \quad (1)$$

where f is the end-effector pose function of joint angle, θ. The Jacobian matrix describes the relationship between the end-effector's pose and each joint variable, approximating the change in the end-effector's pose when a joint variable is altered. This approximate change can be calculated by multiplying the Jacobian matrix, J, with a set of changes in joint variables:

$$\Delta P = J\Delta\theta \quad (2)$$

where ΔP is the change in end-effector's pose and Δθ is set of change in joint variables. To calculate the approximate change in joint variable, Δθ from Equation (2), it is necessary to calculate the inverse Jacobian matrix and the change in joint variables with:

$$\Delta\theta = J^{-1}\Delta P \quad (3)$$

The inverse Jacobian matrix can be easily computed for square matrices. However, for non-square Jacobian matrices, the inverse does not exist. To solve systems with non-square Jacobian matrices, various

methods approximate the inverse, including pseudo-inverse, singular value decomposition, damped least square, and Jacobian transpose. In the pseudo-inverse method, the pseudo-inverse of the Jacobian is expressed as:

$$J^{\dagger} = (J^T J)^{-1} J^T \quad (4)$$

or

$$J^{\dagger} = J^T (J J^T)^{-1} \quad (5)$$

where $J^{\dagger}$ is the pseudo-inverse of Jacobian and J^T is the transpose of Jacobian.

A trajectory describes the time history of a manipulator's end-effector pose and joint positions as it moves through different points. The trajectory planning can be done in Cartesian space or joint space. The Cartesian space is described in terms of position and orientation of the end-effector while the joint space describes the joint values in time domain function. In trajectory planning in joint space, third-order or fifth order polynomial trajectory planning can be used.

B. Review of Previous Works

Mohammed [5] tackled the inverse kinematics of a 7-axis manipulator analytically, introducing a redundancy parameter to exploit its flexibility. This resulted in a computationally efficient, unique closed-form solution. Du et al. [6] employed an iterative method with a closed-loop system to handle the inverse kinematics of a 7-DOF manipulator, using feedback to improve accuracy. They relied on an Unscented Kalman Filter to estimate the system state.

Brandstotter et al. [7] applied a geometric approach by dividing the inverse kinematics problem of a 9-DOF manipulator into three parts: 3R kinematic chain, 3R orthogonal, and 3R spherical wrist problem, respectively. They addressed redundancy through a 'redundancy sphere' concept, defining the space of all possible redundant joint positions for a fixed end-effector position. Lou & Di [8] combined analytical and iterative methods to solve the inverse kinematics of a 2n-DOF manipulator. They

first computed the analytical solution based on the spherical wrist configuration, followed by an iterative method based on Lagrange Multipliers with inequality constraints to solve the remaining equations. Li et al. [9] employed a Jacobian-based iterative method with pseudo-inverse to solve the inverse kinematics of a 5-DOF redundant planar manipulator. They addressed redundancy using a gradient projection method, setting obstacle avoidance as the optimization goal.

Zhou et al. [10] used redundancy parameterization to analytically solve the inverse kinematics of a 7 DOF manipulator. They selected the optimal solution from multiple computed options based on energy optimization that minimizes joint displacement. Safeea et al. [11] proposed a modified damped least squares (DLS) method with singular value decompositions (SVD) to address the non-cyclicity issues that arise in conventional DLS-based inverse kinematics solutions. The non-cyclicity issue occurs when joint angles do not exhibit periodic behavior for periodic end-effector trajectories, such as circular paths.

III. Methodology

A. Software Setup

There are three software used in this project: SolidWorks, Spyder5 IDE, and CoppeliaSim. SolidWorks is used to design and build the 3D model of the 9-DOF serial manipulator. Next, the model of the manipulator is imported into CoppeliaSim, a robotic simulation software, to test its movement. Spyder5 is used to code the robotic kinematics algorithm in Python to control the movement of the robot in CoppeliaSim.

B. Configuration of the 9-DOF serial redundant manipulator

Figure 1 shows the configuration of the 9-DOF serial redundant manipulator. Each of the joints is a revolute joint. The axis of rotation of each joint is orthogonal to the axis of the next joint, except for the second and third joints, whose

axes of rotation are parallel to each other.

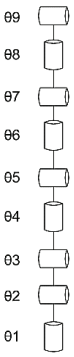

Figure 1: Configuration of 9-DOF serial manipulator

C. Model of 9-DOF Serial Redundant Manipulator

Figure 2 shows the robot model of the 9-DOF serial redundant manipulator in SolidWorks. The model mainly consists of three parts for assembly: the base frame, the manipulator arm with link segments and joints, and the end-effector.

Figure 2: Model of 9-DOF Serial redundant manipulator

D. Forward Kinematics of 9-DOF Serial Manipulator

To simplify the kinematics analysis, the 9-DOF serial manipulator is divided into two parts: a 3-DOF base (joint 1 to joint 3) and a 6-DOF body (joint 4 to joint 9). Figure 3 shows the reference frames assigned for the 3-DOF base, while Table 1 presents the corresponding Denavit-Hartenberg (D-H) parameter.

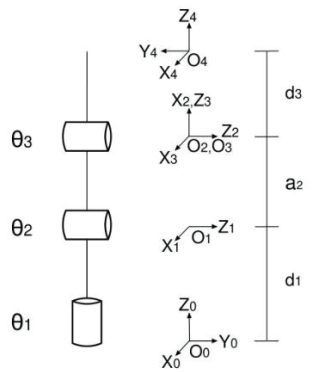

Figure 3: Configuration of 9-DOF serial manipulator

Table 1: D-H parameters for the 3-DOF base

i	$\theta i(rad)$	$di(m)$	$ai(m)$	$\alpha i(rad)$
1	θ_1	d_1	0	$-\pi/2$
2	θ_2	0	a_2	0
3	θ_3	0	0	$\pi/2$
4	0	d_3	0	0

Figure 4 depicts the reference frames assigned for the 6-DOF body, and Table 2 presents the

corresponding Denavit-Hartenberg (D-H) parameters.

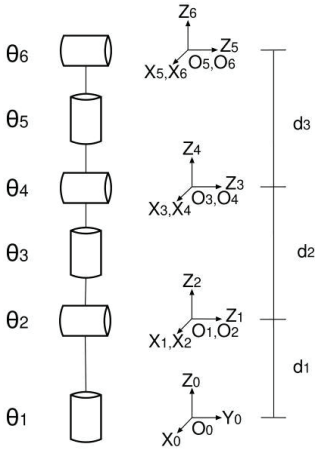

Figure 4: Reference frame for 6-DOF body

Table 2: D-H parameters for 6-DOF body

I	$\theta i(rad)$	$di(m)$	$ai(m)$	$\alpha i(rad)$
1	θ_1	d_1	0	$-\pi/2$
2	θ_2	0	0	$\pi/2$
3	θ_3	d_2	0	$-\pi/2$
4	θ_4	0	0	$\pi/2$
5	θ_5	d_3	0	$-\pi/2$
6	θ_6	0	0	$\pi/2$

E. Inverse Kinematics of 9-DOF Serial Manipulator

The inverse kinematics of the 9-DOF serial redundant manipulator are solved using a Jacobian-based iterative method, with the pseudo-inverse method employed to approximate the inverse of the non-square Jacobian matrix. The 3-DOF base can be solved directly, but the 6-DOF body requires consideration of the position of the last link of the 3-DOF base where it is attached to. Therefore, the 6-DOF body's targeted end-effector pose needs to be shifted according to the calculated pose of its base's last link. Equations (6) and (7) provide the computation of this shifted target end-effector pose.

$$\mathrm{P}_{\mathrm{target2,shifted}} = [\mathrm{R}_{\mathrm{EF1}}]^{-1}[\mathrm{P}_{\mathrm{target2}} - \mathrm{P}_{\mathrm{EF1}}] \quad (6)$$

$$\mathrm{R}_{\mathrm{target2,shifted}} = [\mathrm{R}_{\mathrm{EF1}}]^{-1}[\mathrm{R}_{\mathrm{target2}}] \quad (7)$$

where $P_{target2,shifted}$ is the shifted target position of 6-DOF body, R_{EF1} is the 3×3 rotation matrix of the 3-DOF base, $P_{target2}$ is the 3×1 target position matrix of 6-DOF body, P_{EF1} is the 3×1 position matrix of the 3-DOF base's last link, $R_{target2,shifted}$ is the shifted 3×3 rotation matrix of target of 6-DOF body, and $R_{target2}$ is the 3×3 rotation matrix of target position of the 6-DOF body's end-effector.

For the Jacobian matrix, each column of the Jacobian matrix of 3-DOF base and 6-DOF body

can be calculated by Equation (8).

$$J = \begin{bmatrix} J_v \\ J_\omega \end{bmatrix} = \begin{bmatrix} R_{i-1}^0 \begin{bmatrix} 0 \\ 0 \\ 1 \end{bmatrix} \times (d_n^0 - d_{i-1}^0) \\ R_{i-1}^0 \begin{bmatrix} 0 \\ 0 \\ 1 \end{bmatrix} \end{bmatrix} \quad (8)$$

where R_{i-1}^0 is the rotation matrix from frame 0 to frame $i-1$, d_n^0 is the position vector from frame 0 to frame n, and d_{i-1}^0 is the position vector from frame 0 to frame $i-1$. The value of n is the number of joints and the value of i iterates from 1 to n.

F. Trajectory Planning of 9-DOF Serial Manipulator

To generate the trajectories of motion, point-to-point trajectory planning in Cartesian space was used to form the motion paths for both parts. When given the position of two points, starting point, P_{start} and ending point, P_{end}, the change in position between the points, dP, can be calculated with Equation (9). Each point on the line between these two points can be calculated using interpolation, and this involves dividing the line into many segments and using the inverse kinematic equations to solve the joint angles for each segment.

$$dP = P_{end} - P_{start} \quad (9)$$

Then, given the number of segments, N between the line, each position of point, P_i on the line can be calculated by Equation (10):

$$P_i = P_{start} + \frac{dP}{N} \times i \quad (10)$$

where i is the iteration number that will iterate from 0 to N, the number of segments.

IV. Result and Discussion

A. Results

Figure 5 shows the workspace of the 9-DOF serial manipulator. This workspace is contained within a sphere with a radius of 850 mm. The minimum and maximum reachable positions of the end-effector are -849.89 mm to 849.89 mm along the x and y axes and -605.3 mm to 1004.9 mm along the z-axis.

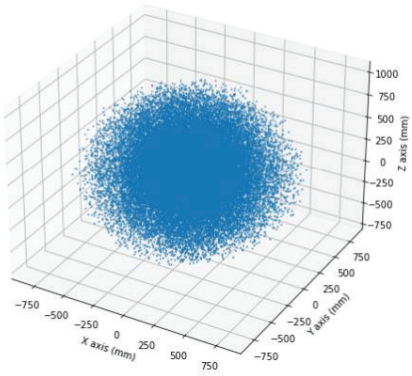

Figure 5: Robot workspace of 9-DOF serial manipulator

In a simulation, the 9-DOF serial manipulator performs a task in a restricted environment. The end-effector follows a specific trajectory while a redundant joint avoids obstacles. Figure 6 shows the initial and final poses of the 9-DOF serial manipulator in this simulation.

In Figure 6, the actual (tracked) trajectories of the redundant links (the 3-DOF base) and the end-effector (the 6-DOF body) are shown as traces labeled *EF_1* and *EF_2*, respectively. The end-effector navigates the narrow space along its targeted trajectory, while the redundant links avoid obstacles simultaneously moving along the S-shaped entry path.

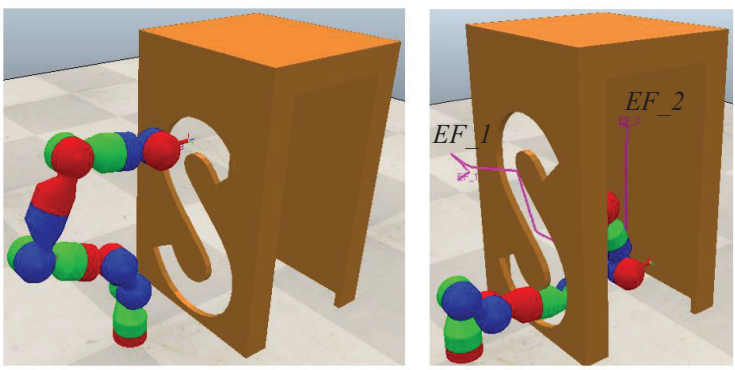

Figure 6: Initial and final pose of 9-DOF serial manipulator

Figure 7 shows the result of the actual (tracked) trajectory of the end-effector labelled with *EF_2* and the targeted trajectory of the end-effector labelled with *Target_2*. Similarly, Figure 8 shows the result of the actual (tracked) trajectory of the redundant links labelled with *EF_1* and the targeted trajectory of the redundant links labelled with *Target_1*.

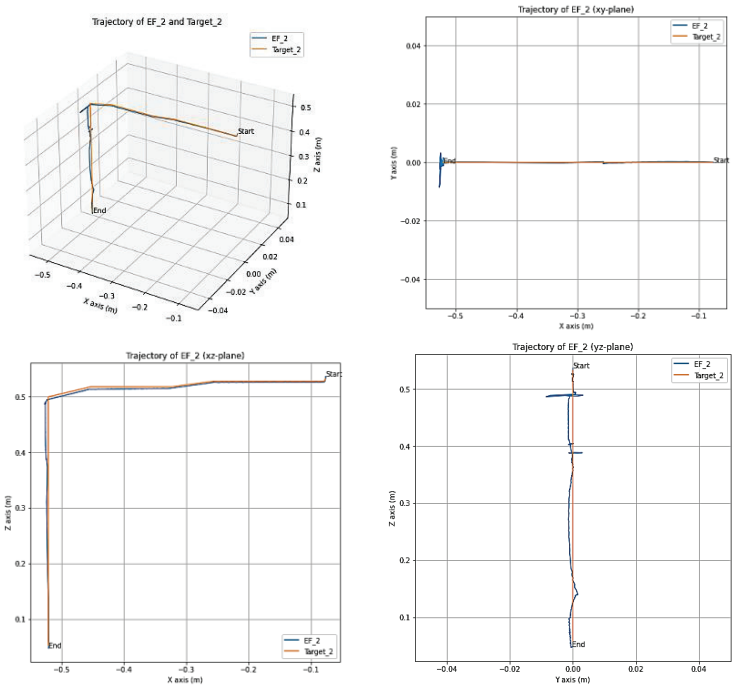

Figure 7: Trajectories of end-effector, *EF_2* and *Target_2*

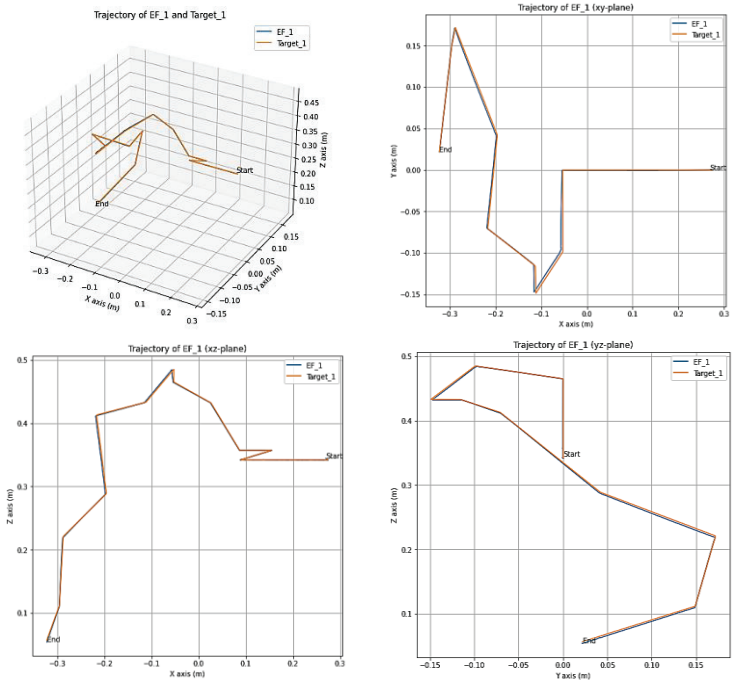

Figure 8: Trajectories of redundant joint, *EF_1* and *Target_1*

The normalized position error between the actual and target trajectory of the end-effector, *EF_2* and redundant links, *EF_1* is recorded as shown in Figure 9. Then, the joint angle value when the 9-DOF serial manipulator moves from the initial pose to the final pose is recorded as shown in Figure 10.

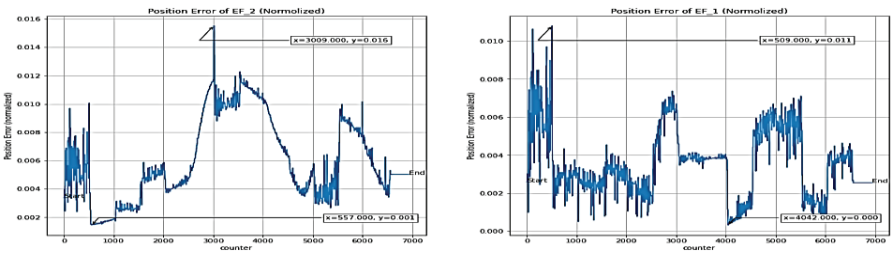

Figure 9: Normalized position error of end-effector, *EF_2* and redundant joint *EF_1*

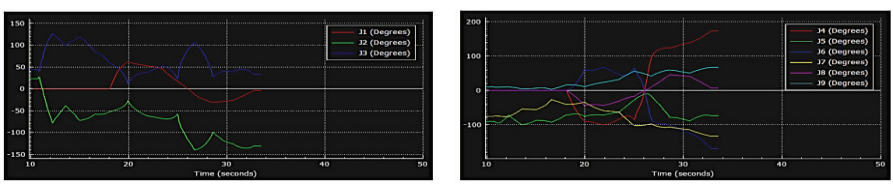

Figure 10: Joint angles for 3-DOF part and 6-DOF body

B. Discussion

To leverage the inherent redundancy of the 9-DOF serial manipulator, the kinematic problem is strategically partitioned into two distinct sections: a 3-DOF base (Joint 1-3) and a 6-DOF body (Joint 4-9). This separation empowers independent control of the redundant joint's position within the 3D Cartesian space via the base, while the body simultaneously governs the end-effector's pose (position and orientation) with its six degrees of freedom. This configuration proves advantageous for several reasons. Firstly, the minimum nine DOFs guarantee simultaneous control of both the end-effector and the redundant joints, a feat impossible for 7-DOF or 8-DOF redundant robots. This expanded controllability allows the manipulator to navigate complex environments

with greater dexterity and adaptability.

Figure 5 further showcases the impressive workspace of the 9-DOF manipulator. The end-effector can reach any point within a generous sphere of 850 mm radius, a significant advantage over its lower-DOF brethren. This expansive reach translates to a substantial operational range, allowing the manipulator to tackle diverse tasks in various environments.

An experiment in simulation has been conducted to demonstrate obstacle avoidance using the redundancy of a 9-DOF serial manipulator. The manipulator performs a specific task in a restricted environment, where the end-effector must follow a trajectory within the narrow space while the redundant links steer clear of obstacles. To achieve this, the redundant links is commanded to move along an S-shaped trajectory that mirrors the entry path to the narrow space, allowing the end-effector to navigate smoothly within the confined area (Figure 6). Figures 7 and 8 show the actual (tracked) and targeted trajectories of both the end-effector and the redundant joint, with minimal error as evidenced by the close proximity of the lines. As shown in the *yz-plane* of Figure 8, the redundant joint's trajectory resembles the S-shaped entry path. Figure 9 further confirms the smooth movement with maximum and minimum normalized position errors for the end-effector at 0.016 and 0.001, respectively, and similar values for the redundant joint.

Finally, Figure 10 reveals the joint angle values for each joint during the manipulator's motion, demonstrating the absence of sudden changes and highlighting the smooth, controlled movement. This experiment showcases the advantage of a 9-DOF robot's redundancy in obstacle avoidance scenarios. The end-effector successfully fulfils its task while adhering to a specific pose, a feat impossible for non-redundant robots like their 6-DOF counterparts.

C. Comparison with Previous Works

It is worth mentioning that the solution proposed in this paper is not limited to a 9-DOF serial redundant manipulator. It serves as a general solution for solving any serial redundant manipulator, regardless of its degrees of freedom, by decomposing the kinematics problem into two or more sub-sections and solving each sub-section individually. In comparison to some of the reviewed prior works, for instance, the 7-DOF robot designed by Mohammed [5], the proposed solution is applicable only to robots with solvable inverse kinematics through redundancy parameterization.

V. Conclusion

In conclusion, this paper proposes a novel solution for both the kinematic modelling and trajectory planning of a 9-DOF serial redundant manipulator. To effectively exploit the robot's redundancy, its kinematic model is divided into two parts: a 3-DOF base (axes 1-3) and a 6-DOF body (axes 4-9). Homogeneous transformation matrices with D-H parameters are used to formulate the forward kinematics of both parts. Subsequently, the inverse kinematics problem is tackled using a Jacobian-based iterative method with the pseudo-inverse approach. Point-to-point trajectory planning in Cartesian space is then employed to generate trajectories for both the base and the arm.

To demonstrate the effectiveness of this approach, an experiment was conducted where the robot's end-effector performs a task in a restricted environment while its redundant links avoid obstacles. The results showcase that both the end-effector and the redundant links can precisely follow their target trajectories with negligible pose errors. This highlights the utility of the proposed solution, particularly in situations where obstacle avoidance is crucial.

VI. References

[1] I. Virgala, M. Kelemen and E. Prada, "Kinematics of Serial Manipulators," *Automation and Control,* 2021.

[2] Y. Bulut and E. S. Conkur, "A real-time path-planning algorithm with extremely tight maneuvering capabilities for hyper-redundant manipulators," *Engineering Science and Technology, an International Journal,* vol. 24, no. 1, p. 247–258.

[3] O. O. Ropo, O. F. Adekunle, O. A. Oluwaseun and O. J. Babatope, "Design of a Pick and Place Serial Manipulator," *IOP Conference Series: Materials Science and Engineering,* vol. 413, no. 1, p. 012056, 2018.

[4] V. V. Chembuly and H. K. Voruganti, "An efficient approach for inverse kinematics and redundancy resolution of spatial redundant robots for cluttered environment," *SN Applied Sciences*, vol. 2, no. 6, 2020.

[5] S. Mohammed, "Kinematic Motion Planning for a 7-Axis Robotic Arm (LWA70 by Schunk)," Master's Thesis, Umeå University, Department of Applied Physics and Electronics, 2016.

[6] H. Du, Y. Zhao, X. Li, J. Han, Z. Wang and G. Song, "A closed-loop framework for inverse kinematics of the 7-DOF manipulator," *Proceedings of 2016 2nd International Conference on Control Science and Systems Engineering, ICCSSE 2016,* pp. 237-241, 2016.

[7] M. Brandstotter, S. Muehlbacher-Karrer, D. Schett and H. Zangl, "Virtual compliance control of a kinematically redundant serial manipulator with 9 DoF," *Advances in Intelligent Systems and Computing,* vol. 540, pp. 38-46, 2017.

[8] Y. Lou and S. Di, "A Hybrid Inverse Kinematics for 2n-DOF Redundant Manipulator Based on General SphericalWrist," *2018 2nd International Conference on Robotics and Automation Sciences, ICRAS 2018,* pp. 117-122, 2018.

[9] J. Li, Y. Liu and X. Zang, "Kinematics Ayalysis for a Heavy-load Redundant Manipulator Arm Based on Gradient Projection Method," *Proceedings of 2018 IEEE 3rd Advanced Information Technology, Electronic and Automation Control Conference, IAEAC 2018*, pp. 260-264, 2018.

[10] S. Zhou, H. Liu, C. Jiang, H. Du, Y. Gan and Z. Chu, "Research on Kinematics Solution of 7-axis Redundant Robot Based on Self-motion," *Proceedings - 2020 Chinese Automation Congress, CAC 2020*, p. 2622–2627, 2020.

[11] M. Safeea, R. Bearee and P. Neto, "A Modified DLS Scheme with Controlled Cyclic Solution for Inverse Kinematics in Redundant Robots," *IEEE Transactions on Industrial Informatics,* vol. 17, no. 12, p. 8014–8023, 2021.